RAMAN AND LUMINESCENCE SPECTROSCOPY OF MANGANESE MINERALS: PREPARING FOR SUPERCAM, MARS 2020. A. M. Ollila[1], N. L. Lanza[1], O. Beyssac[2], M. Gauthier[2], S. Clegg[1], A. Misra[3], S. Sharma[3], R. C. Wiens[1], S. Maurice[4], O. Gasnault[4], [1]Los Alamos National Laboratory, Los Alamos, NM (amo@lanl.gov), [2]IMPMC, Sorbonne Universités, Paris, France, [3]University of Hawaii, Honolulu, HI, [4]IRAP, Toulouse, France.

Introduction: Numerous occurrences of high manganese concentrations (>3 wt. % MnO) have been observed by ChemCam on the Mars rover Curiosity in Gale crater [1,2,3]. Elevated Mn has also been seen by APXS in Endeavour crater by the Opportunity rover [4], indicating a widespread distribution. These chemistry observations provide important clues pointing toward habitable aqueous environments with highly oxidizing conditions. However, mineralogical context for the Mn deposits is critical to understanding the environmental conditions under which the minerals formed. Unfortunately, these deposits have not been analyzed by a mineralogical tool. CheMin, an X-ray diffratometer on Curiosity, has not analyzed these materials because to date they have been identified either within thin fracture fill layers [2] or the matrix of fine-grained sediments [1], both of which are challenging to input to CheMin in significant quantities.

The Mars 2020 rover will have two instruments capable of mineralogical analyses of these challenging materials. SuperCam and SHERLOC use Raman spectroscopy to identify minerals based on characteristic molecular and lattice vibrations. SuperCam can also analyze luminescence emission induced by trace element substitutions. Here we focus on SuperCam's ability to identify high Mn minerals using Raman and luminescence spectroscopy.

Samples: A suite of natural rock samples containing Mn minerals were analyzed by Raman and luminescence spectroscopy. A list of minerals is provided in [5]; mineralogy has been confirmed by XRD except where noted here. These include (1) a biogenic marine nodule from Chesapeake Bay, which is composed of todorokite, romanechite, and birnessite (all mixed valence hydrated Mn-oxides with variable Na, Ca, K, and Ba); (2) pyrolusite ($Mn^{4+}O_2$); (3) psilomelane (or cryptomelane), which is composed of minerals such as hollandite and romanechite; (4) manganite ($Mn^{3+}O(OH)$); (5) hausmannite (not confirmed by XRD, $Mn^{2+}Mn^{3+}{}_3O_4$); and (6) rhodochrosite ($Mn^{2+}CO_3$). An additional Pacific Ocean nodule has been added to this list but mineralogy has not been confirmed by XRD.

Methods: Samples were analyzed by Raman and luminescence spectroscopy at the Institut de Minérelogie, de Physique des Matériaux et de Cosmochimie at Sorbonne Universités in Paris, France. This system, like SuperCam, uses a pulsed 532 nm laser synchronized with a gated intensified CCD. Unlike SuperCam, sample analysis is conducted through a microscope with a spatial resolution of ~90 μm and is capable of both low and high spectral resolution modes (2-12 cm^{-1} FWHM), whereas SuperCam will operate from 1.5 to 12 m from the rover with a spatial resolution of ~1-3 mm and a spectral resolution of 8-12 cm^{-1} FWHM. Here, to improve signal to noise, between 20,000 and 200,000 spectra were added together; SuperCam will likely obtain <200 spectra per point to conserve resources. A diamond, which has a strong Raman peak at ~1332 cm^{-1}, was used to optimize the delay and gate width. The gate width for Raman and luminescence analyses were 4.5 to 5 ns and 0.45 ms, respectively.

Results and Discussion: Raman spectra collected on these minerals are consistent with database spectra from RRUFF [6]. RRUFF spectra have been background corrected whereas our data has only had a non-laser "dark" subtraction applied to it. Fig. 1 illustrates some of the more difficult minerals to identify via Raman. The Chesapeake nodule contains todorokite, romanechite, and birnessite (birnessite spectrum not available on RRUFF), and it appears that the other ocean nodule and psilomelane likely also contain these minerals as well. Birnessite spectra from [7] also strongly resemble these spectra, indicating there will be difficulty distinguishing this suite of minerals. The broadness of the bands in the ocean nodules indicates the presence of micro-crystalline material.

Fig. 2 compares RRUFF database spectra of hausmannite, manganite, pyrolusite, and rhodochrosite.

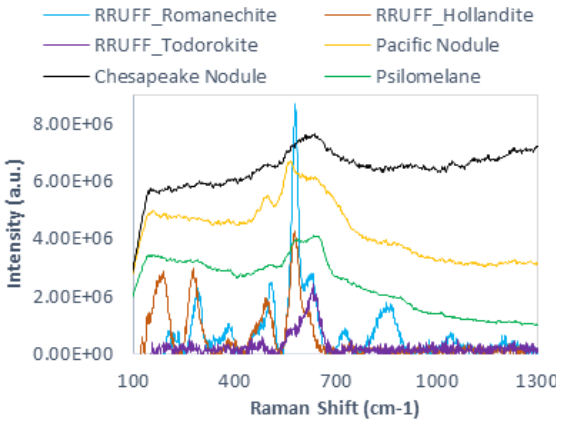

Fig. 1: Raman spectra of two ocean nodules compared to RRUFF spectra of romanechite, hollandite and todorokite.

With the exception of pyrolusite, which required high spectral resolution analysis to see the primary Raman peak, this group of Mn minerals should be straightforward to identify with Raman spectroscopy.

Luminescence spectroscopy revealed a broad feature centered at ~650 nm (3430 Raman shift cm^{-1}) attributable to Mn^{2+} in rhodochrosite [8] and both broad and sharp features around ~694 nm (Fig. 3). While the Fluomin database [8] does not list any luminescence centers around 694 nm for these minerals, this region is where Cr^{3+} luminescence is observed in minerals like ruby, spinel, and topaz [8]. The R1 and R2 lines of Cr^{3+} in ruby occur at 694.3 and 692.9 nm, respectively, and the peak centers for the psilomelane doublet occur very close to these values at 694.4 and 693.0 nm. Further analysis is required to determine if there is a Cr impurity in these samples that is inducing these features.

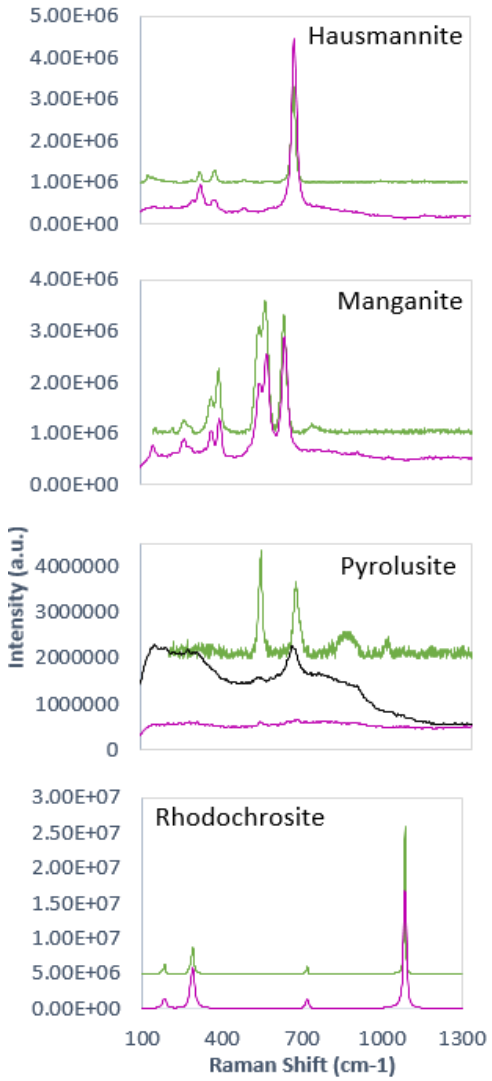

Fig. 2: Raman spectra of four Mn minerals. Upper spectrum (green) in each plot is from the RRUFF database. Purple and black spectra were collected on a microscope benchtop instrument at IMPMC. For pyrolusite, the black spectrum was taken with a higher resolution grating than the purple spectrum.

Conclusions: Minerals such as romanchite, todorokite, birnessite, and pyrolusite are somewhat difficult to distinguish via Raman spectroscopy but hausmannite, manganite, and rhodochrosite have more readily distinguishable diagnostic peaks. Luminescence features attributable to Mn^{2+} were identified in rhodochrosite and unknown luminescence was seen in several other minerals; this luminescence will be further investigated to determine its origin. These spectra will be used to compare to SuperCam data that will be collected this spring using the Engineering Qualification Unit.

References: [1] Lamm S., et al. (2018) LSPC [2] Lanza N. L., et al. (2016) GRL 43, 7398-7407. [3] Gasda P., et al. (2018) LPSC. [4] Arvidson R. et al. (2016) Am. Mineralogist 101(6), 1389-1405. [5] Lanza N. L. et al. (2017) LPSC, 2913. [6] RRUFF Database, rruff.info. [7] Buzgar N. et al. (2013) J. Archaeological Sci. 40, 2128-2135. [8] Luminescent Mineral Database and Information, www.fluomin.org.

Acknowledgements: This work was supported by a LANL Laboratory Directed R & D Early Career Award and a Director's Postdoctoral Fellowship. The IMPMC setup is supported by Sorbonne Universités, CNRS and CNES.

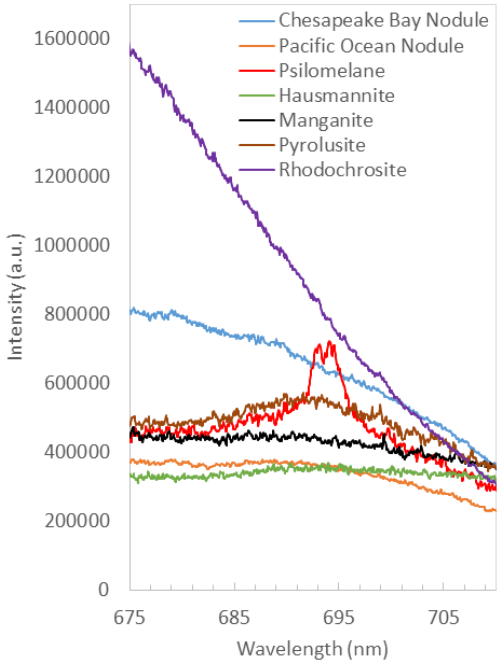

Fig. 3: Luminescence spectra of the 694 nm region (~4400 cm^{-1} Raman shift) illustrating unidentified luminescence, potentially attributable Cr^{3+}.